ORIGINAL ARTICLE
Neuroscience

JKMS

http://dx.doi.org/10.3346/jkms.2012.27.3.291 • J Korean Med Sci 2012; 27: 291-299

Increased Expression of EMMPRIN and VEGF in the Rat Brain after Gamma Irradiation

Ming Wei[1,*], Hong Li[1,*], Huiling Huang[2], Desheng Xu[1], Dashi Zhi[2], Dong Liu[1], and Yipei Zhang[1]

[1]Department of Neurosurgery, the Second Hospital of Tianjin Medical University, Tianjin; [2]Department of Neurosurgery, Tianjin Huanhu Hospital, and Tianjin Neurosurgery Institute, Tianjin, China

*Ming Wei and Hong Li contributed equally to this work.

Received: 20 August 2011
Accepted: 2 December 2011

Address for Correspondence:
Hong Li, MD
Department of Neurosurgery, the Second Hospital of Tianjin Medical University, 23 Pingjiang Road, Tianjin - 300211, China
Tel: +86-22-88328537, Fax: +86-22-28331788
Email: neuroli@126.com

This study was supported in part by grants-in-aid for scientific research from the Tianjin Bureau of Public Health, Tianjin, China (grant: 06KZ25, 2010KZ92).

The extracellular matrix metalloproteinase inducer (EMMPRIN) has been known to play a key regulatory role in pathological angiogenesis. A elevated activation of vascular endothelial growth factor (VEGF) following radiation injury has been shown to mediate blood-brain barrier (BBB) breakdown. However, the roles of EMMPRIN and VEGF in radiation-induced brain injury after gamma knife surgery (GKS) are not clearly understood. In this study, we investigated EMMPRIN changes in a rat model of radiation injury following GKS and examined potential associations between EMMPRIN and VEGF expression. Adult male rats were subjected to cerebral radiation injury by GKS under anesthesia. We found that EMMPRIN and VEGF expression were markedly upregulated in the target area at 8-12 weeks after GKS compared with the control group by western blot, immunohistochemistry, and RT-PCR analysis. Immunofluorescent double staining demonstrated that EMMPRIN signals colocalized with caspase-3 and VEGF-positive cells. Our data also demonstrated that increased EMMPRIN expression was correlated with increased VEGF levels in a temporal manner. This is the first study to show that EMMPRIN and VEGF may play a role in radiation injuries of the central nervous system after GKS.

Key Words: EMMPRIN; Immunohistochemistry; Radiosurgery; Radiation Injuries, Experimental; Vascular Endothelial Growth Factor

INTRODUCTION

The field of gamma knife surgery (GKS) is expanding in the treatment of central nervous system disorders (1, 2). Radiation injury to the brain may lead to severe complications from acute, early and late reactions. Varying degrees of vascular changes including the modification of vascular structure and alterations in permeability can contribute to this pathological response (3). However, there are very limited data on the role of modifying factors associated with angiogenesis and vascular remodeling.

Extracellular matrix metalloproteinase inducer (EMMPRIN) is a cell surface transmembrane glycoprotein that contains two extracellular immunoglobulin domains (C and V) and belongs to the immunoglobulin superfamily (4). EMMPRIN is known for its ability to induce matrix metalloproteinase (MMP) production (5), which degrades the basement membrane of the original vessel and remodels the extracellular matrix (ECM) around neurovasculature sites. Recent studies have demonstrated that overexpression of EMMPRIN plays a critical role in myocardial and renal injury induced by ischemia and reperfusion (6, 7). EMMPRIN has been reported to be associated with the pathogenesis of cerebral disorders such as ischemia and stroke, multiple sclerosis, and Alzheimer's disease (8-10); however, no data are available that elucidate the role of EMMPRIN in radiation injury. Various cytokines and growth factors have been shown to enhance the activities of EMMPRIN, such as epidermal growth factor (11) and transforming growth factor (12), and these cytokines (potentially capable of influencing EMMPRIN expression) have been reported to be increased within irradiated tissues (13). We therefore hypothesized that EMMPRIN expression in the irradiated brain can be upregulated and thus contribute to radiosurgically induced vascular injury.

VEGF is a member of a family of angiogenesis-related growth factors. It is a highly conserved 36-46 kDa dimeric glycoprotein with potent and specific activity in promoting endothelial cell proliferation and vascular permeability. VEGF-induced increases in microvessel permeability have been demonstrated not only in normal brain endothelial cells but also in disease conditions, such as in tissues surrounding brain tumors (14) and ischemia lesions (15). Previous studies have found radiation-induced increases of VEGF expression in regions of blood-spinal cord barrier disruption after conventional radiotherapy (16). However, the radiobiological changes associated with radiosurgery are not the same as those observed in conventional radiotherapy with lower doses of radiation, and dynamic changes of VEGF after GKS in vivo have yet to be studied.

pISSN 1011-8934
eISSN 1598-6357

The aforementioned experimental results prompted us to investigate whether EMMPRIN and VEGF play important roles in radiosurgery-induced vascular disturbances. In the current study, the effect of GKS on the expression of EMMPRIN and VEGF was examined in the rat brain.

MATERIALS AND METHODS

Animal protocol

A total of ninety-six male Wistar rats weighing between 200 and 240 g were housed individually in a temperature- (22°C) and humidity-controlled (60%) vivarium and maintained on a standard 12-hr light/dark cycle (7:00 a.m. to 7:00 p.m. per cycle) with free access to food and water. The rats were randomly assigned to control and GKS groups (48 rats per group). Four time points at 1, 4, 8, and 12 weeks after irradiation or sham-irradiation were analyzed for each study group. Experiments involving animals were approved by the Tianjin Medical University Animal Care and Ethics Committee.

Gamma Knife surgery

The radiation target and dosage were determined based on studies described previously (17). Briefly, each rat was anesthetized with 10% chloraldurat (3 mL/kg), and its head was fixed in a stereotactic brain frame. After high-resolution MR images were obtained, the center of the irradiation area was calculated with reference to a standard rat stereotactic atlas (X = 5, Y = 10, Z = 6.5). A maximum dose of 75 Gy was administered in the right parietal cortex with a Leksell Gamma Knife (model C, Elekta Instrument AB , Stockholm, Sweden) using a 4-mm collimator. The control animals were identically manipulated but did not receive any radiation.

Histology and immunohistochemistry

The rats were perfused transcardially with 4% paraformaldehyde under intraperitoneal anesthesia; the brains were then removed and post-fixed overnight at 4°C in 4% paraformaldehyde. The brains were cut at the target region and embedded in paraffin. A series of 4-μm thick paraffin sections were cut and mounted on the slides for further hematoxylin and eosin or immunohistochemical staining. The sections were treated with standard 1.5% horse or goat serum for 30 min, followed by an overnight incubation at 4°C with goat polyclonal anti-EMMPRIN (1:100; Santa Cruz Biotechnology, Santa Cruz, CA, USA) and mouse monoclonal anti-VEGF (1:100; Santa Cruz Biotechnology). After incubation with diluted biotinylated secondary antibody, the sections were incubated with ABC Reagent (Vector Laboratories, Burlingame, CA, USA) for 30 min, and visualized using 0.05% diaminobenzidine for 5-10 min. The positive cells were quantified from 10 random × 400 fields in a blinded fashion. An isotype-matched negative control was used for all the antibodies.

Transmission electron microscopy

After perfusion, the parietal cortical tissue specimens at the sites of radiation were immediately excised. The radiation target was identified using the method previously described (17). Tissue blocks (1 μL) were excised and immersed in a fixative solution of 2% paraformaldehyde and 2.5% glutaraldehyde in 0.1 M/L phosphate buffer. The samples were dehydrated in a series of ethanol and transferred to 100% propylene oxide for 15 min, followed by graded resin infiltration and embedding. Ultrathin sections were prepared on a Leica Ultracut using a 45-degree diamond histoknife, and images were captured using a Hitachi H7650 Transmission Electron Microscope.

Water content analysis by dry/wet weight measurements

After the irradiated parietal cortices were carefully dissected, the tissues were weighed immediately and dried under vacuum for up to 2 weeks. The weights were measured throughout the drying period until no further change occurred. Water content was calculated as follows: Water content = (wet weight-dry weight)/wet weight 100 (%).

Evans blue (EB) extravasation

A 2% (w/v) solution of EB at 4 mL/kg was injected intravenously and allowed to circulate for 30 min. The brain EB extravasation was quantified spectrophotometrically. The brains were homogenized by vortexing in 250 μL of phosphate-buffered saline (PBS) for 2 min. Then, 250 μL of 60% trichloroacetic acid was added, and the samples were vortexed for 2 min. After cooling for 30 min, the samples were centrifuged for 5 min at 10,000 g. Absorbance readings were measured at 620 nm. EB extravasation results are expressed as ng of EB per mg of brain tissue. For qualitative examination of EB extravasation, the rats were perfused with 5 mL of saline followed by 5 mL of 4% paraformaldehyde. The removed brains were immersed in 30% sucrose in 0.1 M PBS for 48 hr, frozen in OCT (Sigma Chemical Co., St. Louis, MO, USA), and stored at -80°C. The EB extravasation was observed in the cryostat sections (14 μm) using a fluorescent microscope.

Western blot analysis

Expression of EMMPRIN and VEGF protein was monitored at the indicated time points by Western blotting. The injured brain tissue was collected and homogenized with RIPA buffer containing protease inhibitors cocktail (Sigma), and then incubated for 15 min on ice. The supernatant was isolated by centrifugation at 12,000 g for 20 min at 4°C. The concentration of total protein in each sample was quantitated by Bradford method (Bio-Rad, Hercules, CA, USA), as per the manufacturer's instructions. Equal amounts of proteins were separated by SDS–PAGE, and then transferred to polyvinylidene difluoride membranes (Immobilon-P; Millipore, Billerica, MA, USA) for 1 hr. The membrane

http://dx.doi.org/10.3346/jkms.2012.27.3.291

was blocked for 1 hr and incubated with goat polyclonal anti-EMMPRIN (1:200; Santa Cruz Biotechnology, Santa Cruz, CA) and mouse monoclonal anti-VEGF (1:200; Santa Cruz Biotechnology) in blocking solution at 4°C overnight. After triple washing, the membrane was incubated with horseradish peroxidase-conjugated secondary antibody (1:2,000) at room temperature for 2 hr. In order to confirm equal protein loading, the blots were also reacted with antibodies against β-actin (Santa Cruz Biotechnology; 1:1,000). The target protein was detected using the ECL + kit (Millipore).

Dual fluorescent staining

For double-immunofluorescence labeling, the cryostat sections were incubated with goat polyclonal antibody to EMMPRIN and mouse monoclonal antibody to VEGF or rabbit polyclonal antibody to caspase-3 (Chemicon, San Diego, CA, USA) overnight at 4°C. All slides were then washed repeatedly in PBS. Subsequently, the sections were incubated with the appropriate secondary antibody conjugated with fluorescent dyes (Alexa Fluor 594 or Alexa Fluor 488; Molecular Probes, Inc., Eugene, OR, USA). The slides were visualized under a fluorescent microscope. In the negative controls, the primary antibody was substituted with PBS.

Statistical analysis

Data are expressed as the mean ± standard deviation (SD). Comparisons among multiple groups were performed using analysis of variance (ANOVA) with Dunnett's post hoc tests. Comparisons between the two treatment groups were made using Student's t-test. The correlation between VEGF and EMMPRIN expression was analyzed using linear regression analysis. A P value of less than 0.05 was considered to be statistically significant.

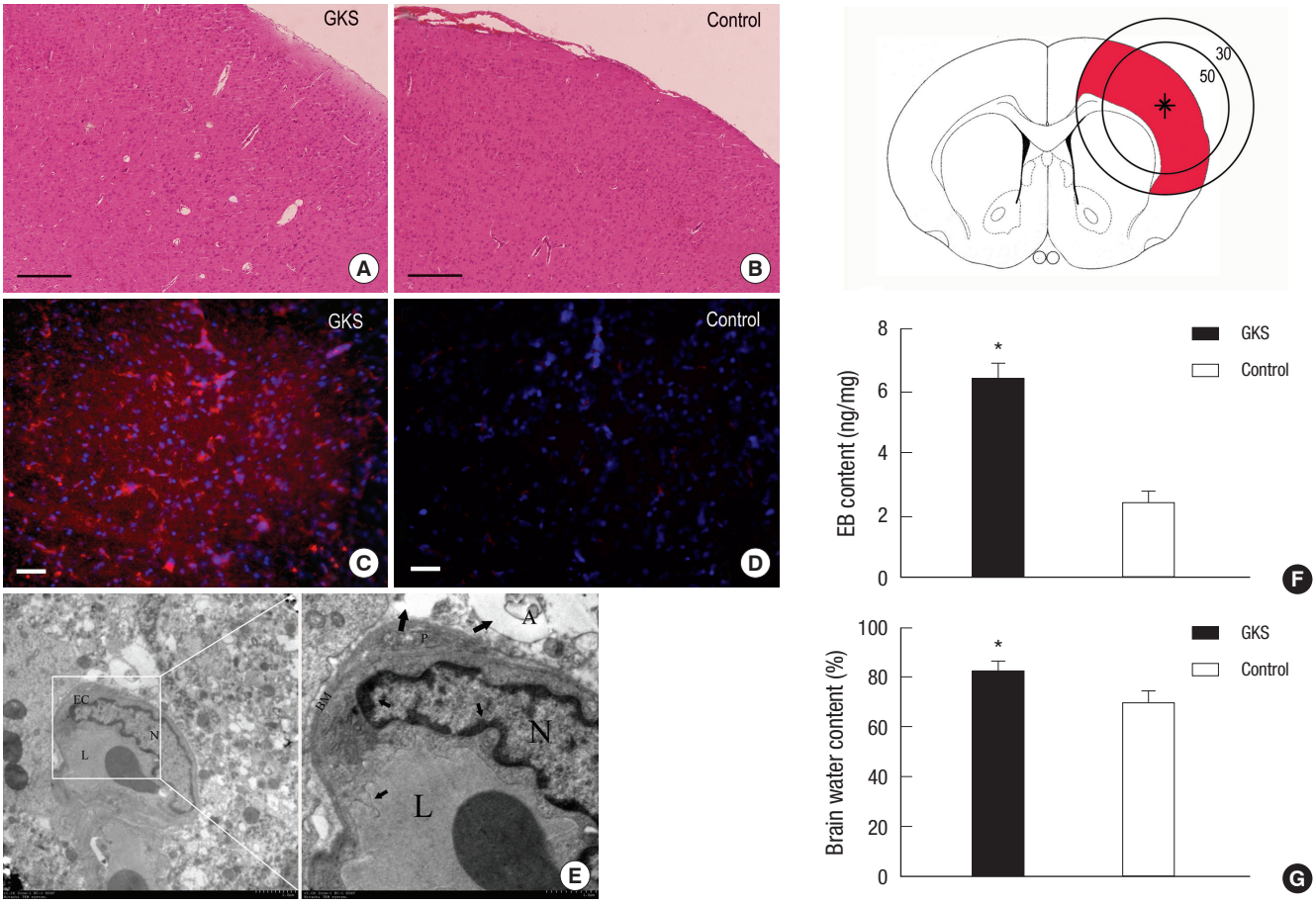

Fig. 1. Radiation damage observed 12 weeks after irradiation. Upper left, drawing of a coronal section of the rat brain showing the isodose curve with a maximal center dose of 75 Gy. (**A** and **B**) Photomicrographs of coronal sections stained with hematoxylin/eosin are shown from the irradiated (**A**) and nonirradiated (**B**) cortex. Enlarged vessels were observed in GKS-irradiated regions. Scale bar = 250 μm. (**C**, **D**, and **E**) EB extravasation in the target region. The significant EB fluorescence (red) was observed in the target region (**C**). There was no EB fluorescence detected in the nonirradiated cortex (**D**). Scale bar = 50 μm. The EB concentration in the irradiated tissue was significantly higher than in the sham-operated group (**F**). (**E**) Ultrastructural observations of brain capillary endothelial cells. Changes included the enlargement of endothelial nuclei, pykno-chromatin (short arrow), process of the plasma membrane (short arrow) and astroglial edema (long arrow). A, astrocyte; EC, endothelial cell; N, nuclei; L, capillary lumen; BM, basement membrane. (**F**) The brain water content in the parietal cortex increased in GKS groups compared with the controls. The data are presented as the mean ± SD. *$P < 0.001$ compared with the sham-operated group.

RESULTS

Radiation-induced histological changes in brain tissue

In the present study, the parietal cortex was the target of unilateral irradiation and the site of microscopic analyses. H&E staining and electron microscopy showed evidence of injury in brain tissue 12 weeks after irradiation (Fig. 1). The histological changes were characterized by dilation of vessels, swelling of endothelia cells and astrocytes, chromatin condensation and aggregation, and destructive changes in membranous structures. Meanwhile, an increase in EB content and brain water content was also observed in irradiated tissue compared with the sham controls (6.64 ± 0.24 vs 2.42 ± 0.36 and 81.18 ± 0.57 vs 70.05 ± 0.95, respectively; $P < 0.001$). Necrosis was not observed in the irradiated brain tissues, and no lesions were observed in the unirradiated controls.

Effects of GKS on expression of EMMPRIN in the rat brain

Immunohistochemical analysis of paraffin-embedded sections for EMMPRIN showed that in the parietal cortex, EMMPRIN was mainly observed in microvessel-like structures (Fig. 2). No significant differences were detected between the GKS and sham control groups at 1 and 4 weeks after GKS ($P = 1.00$). The number of EMMPRIN-positive cells was significantly higher at 8 and 12 weeks after GKS compared with the controls (7.25 ± 1.71 vs 3.50 ± 1.00 and 11.00 ± 1.83 vs 3.75 ± 0.50; $P < 0.001$ for 8 and 12 weeks compared with the injury controls).

Western blot analysis showed that the EMMPRIN was detected as an immunoreactive band with a mean apparent molecular mass of approximately 50 kDa (Fig. 2). There was a significant increase in EMMPRIN protein expression in the irradiated cortex after 8 weeks compared with the controls (0.54 ± 0.03 vs 0.20 ± 0.02; $P < 0.001$) and was sustained at a higher level (0.70 ± 0.01 vs 0.21 ± 0.02; $P < 0.001$) at 12 weeks after GKS.

Real-time PCR was used to determine the gene expression of EMMPRIN in the control and GKS groups (Fig. 3). EMMPRIN levels significantly increased in rats subjected to GKS compared with the sham control group ($P < 0.001$) at 8 and 12 weeks post-radiation. EMMPRIN levels did not differ significantly in both groups at 1 and 4 weeks post-radiation ($P = 0.78$ and $P = 0.85$).

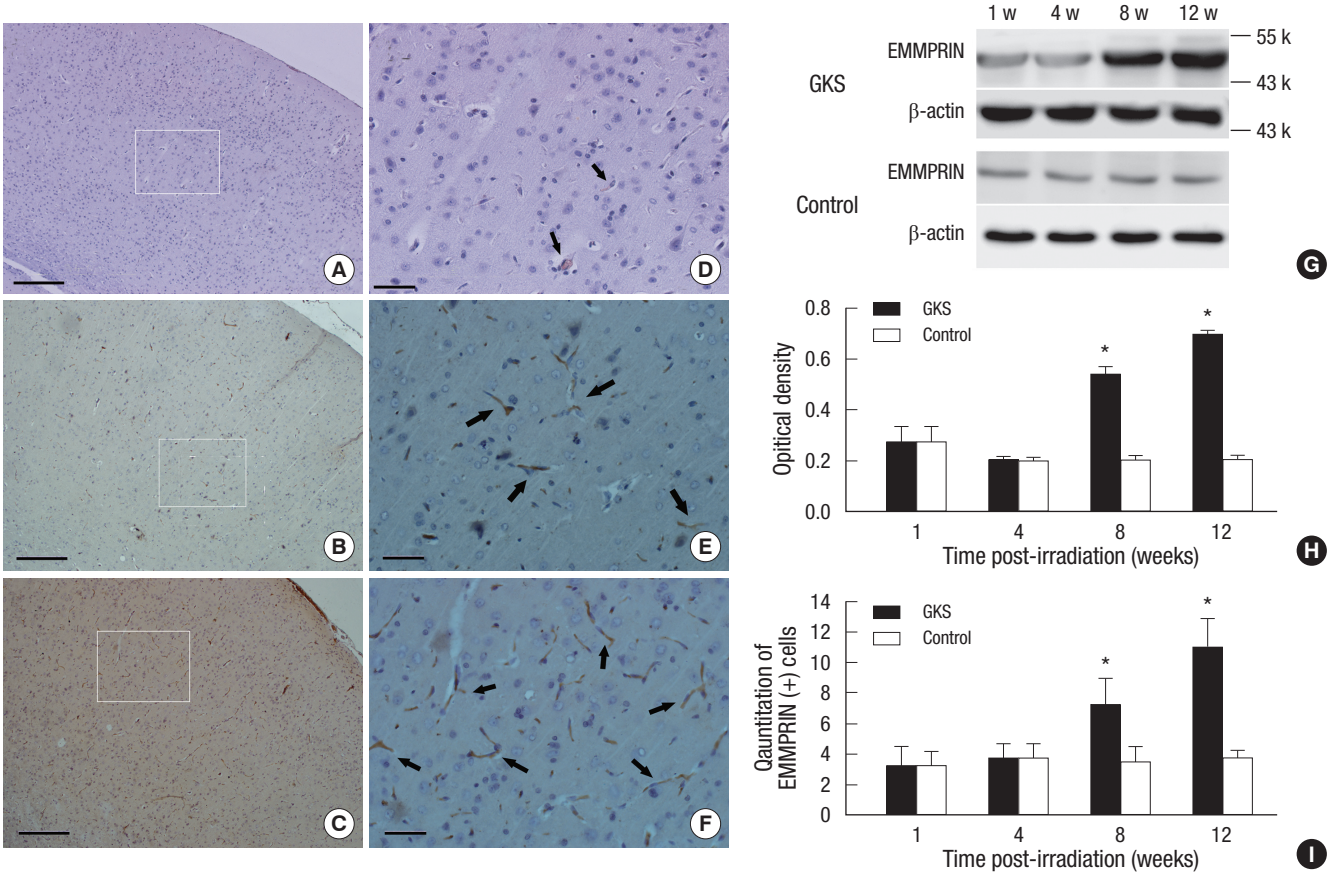

Fig. 2. Immunodetection of EMMPRIN after GKS. (**A**-**F**) Representative photomicrographs of EMMPRIN immunostaining in GKS-irradiated regions. Low baseline levels of EMMPRIN are observed in the sham-operated rat cortex (**A**), whereas EMMPRIN staining increases compared with the sham control at 8 and 12 weeks after GKS (**B**, **C**). (**D**-**F**) Higher magnification image of EMMPRIN signal. Arrows indicate positive EMMPRIN signal. Scale bar = 250 μm (**A**-**C**), or 50 μm (**D**-**F**). (**G**) Immunoblot of EMMPRIN protein expression in the damaged cortex after GKS. Bar graph shows the densitometric analysis of EMMPRIN-immunoreactive bands (**H**) and the temporal change of EMMPRIN-expressing cells after GKS (**I**). The data are presented as the mean ± SD. *$P < 0.001$ compared with the sham group.

http://dx.doi.org/10.3346/jkms.2012.27.3.291

Effects of GKS on expression of VEGF in the rat brain

Immunohistological staining showed that the number of VEGF-positive cells increased in the irradiated right parietal cortex at 8 and 12 weeks after GKS (12.75 ± 2.22 and 18.50 ± 1.73, $P <$ 0.001; Fig. 4). By comparison, the number of VEGF-positive cells was low in brain tissues taken from the control rats (6.00 ± 1.41 and 6.25 ± 1.50).

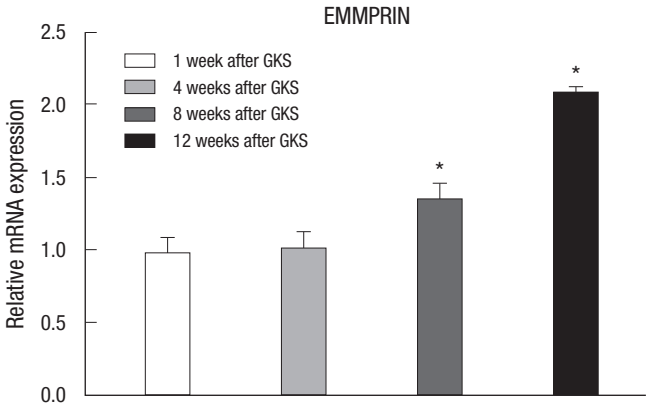

Fig. 3. Quantitative PCR analysis for EMMPRIN in the cortex ipsilateral to the irradiation at 1, 4, 8, and 12 weeks after GKS. The average mRNA expression level in the sham brains was set to 1. Histogram and bars represent the mean ± SD of three replicas. *$P <$ 0.001 compared with the sham group.

To further examine the upregulation of VEGF, proteins obtained from homogenates of the rat brain tissue were used for western blot analysis. VEGF was visualized as a 21-kDa band, and VEGF protein contents were significantly higher in rats treated with GKS compared with the control rats at 8 and 12 weeks after GKS (0.510 ± 0.01 vs 1.94 ± 0.01 and 0.621 ± 0.02 vs 0.197 ± 0.01; $P <$ 0.001; Fig. 4). There was no difference between the rats in the radiation groups and the control rats at 1 and 4 weeks after GKS ($P = 0.66$ and $P = 0.51$).

Using real-time PCR analysis, VEGF mRNA from irradiated brain tissue was examined at 1, 4, 8, and 12 weeks after irradiation and compared with the sham-irradiated controls. We detected a statistically significant increase in VEGF mRNA ($P <$ 0.001; Fig. 5) in the irradiated brain tissue compared with the control brain tissue at 8 and 12 weeks after irradiation. At 1 and 4 weeks post irradiation, both the control and irradiated brain tissues expressed approximately equal levels of VEGF mRNA

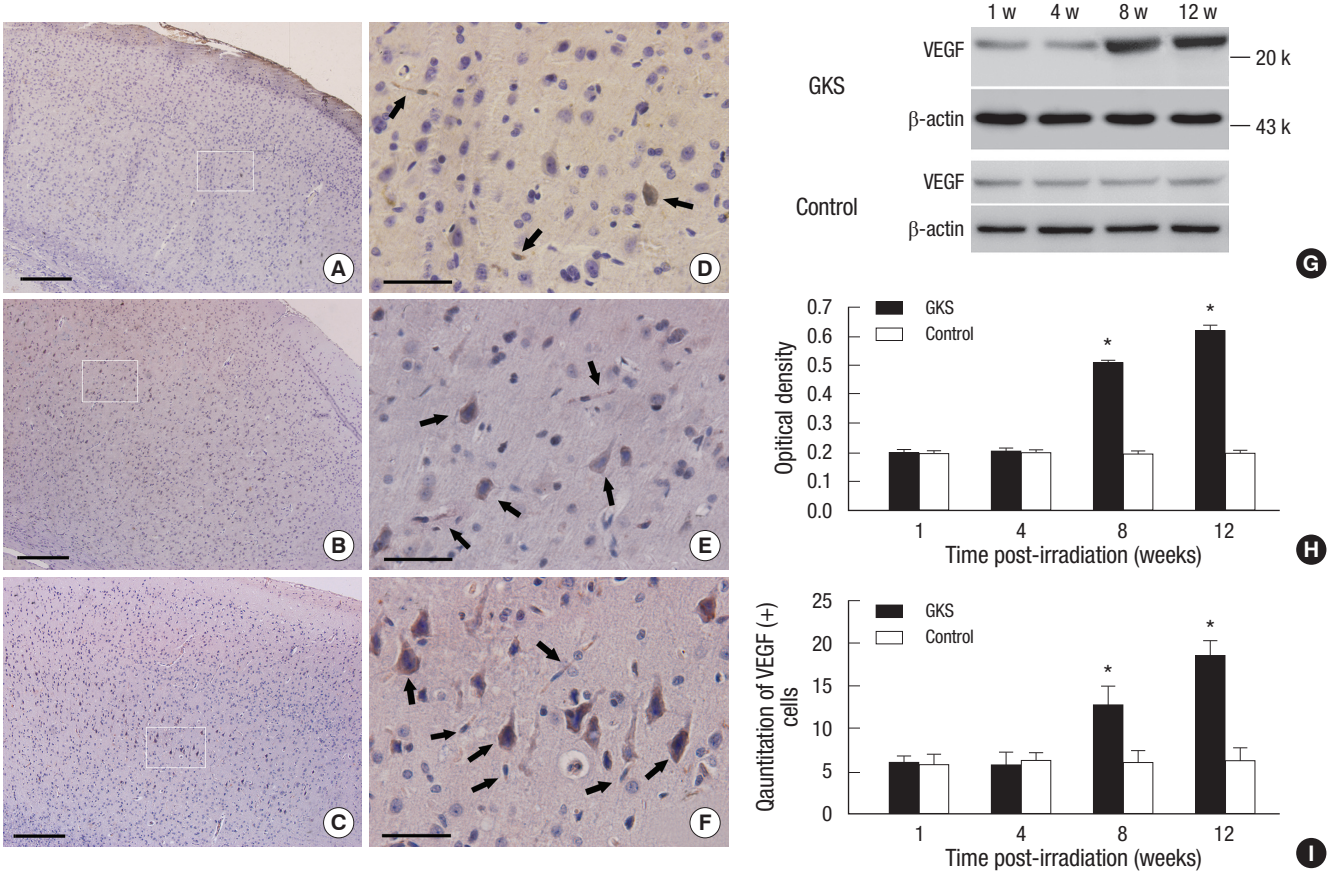

Fig. 4. Immunodetection of VEGF after GKS. (**A**-**F**) Representative photomicrographs of VEGF immunostaining after GKS. A few cells in the cortex of sham-operated rats are VEGF-positive (**A**). However, significant increases in expression of the VEGF occur in the irradiated cortex at 8 and 12 weeks after GKS (**B**, **C**). (**D**-**F**) Higher magnification image of the VEGF signal. Arrows indicate positive VEGF signal. Scale bar = 250 μm (**A**-**C**), or 50 μm (**D**-**F**). (**G**) Immunoblot analysis of VEGF protein expression in the damaged brain tissues 1 to 12 weeks after GKS. Bar graph shows the densitometric analysis of VEGF-immunoreactive bands (**H**) and the temporal change of VEGF (+) cells (**I**) after GKS. The data are presented as the mean ± SD. *$P <$ 0.001 compared with the sham group.

($P = 0.71$ and $P = 0.30$).

Co-localization of EMMPRIN and caspase-3 expression in the parietal cortex after GKS

Caspase-3 is a key factor leading to apoptosis and is often used as a marker of apoptosis. To determine if cells expressing EMMPRIN were undergoing caspase-3 activation after GKS, double-fluorescence immunohistochemistry was used to detect the expression of EMMPRIN and caspase-3 on frozen sections. The overlap of signal between EMMPRIN and caspase-3 was observed in the injured cortex from rats subjected to irradiation. In the control group, there were only a few caspase-3-positive cells in the corresponding region, and these cells were not immunopositive for EMMPRIN (Fig. 6).

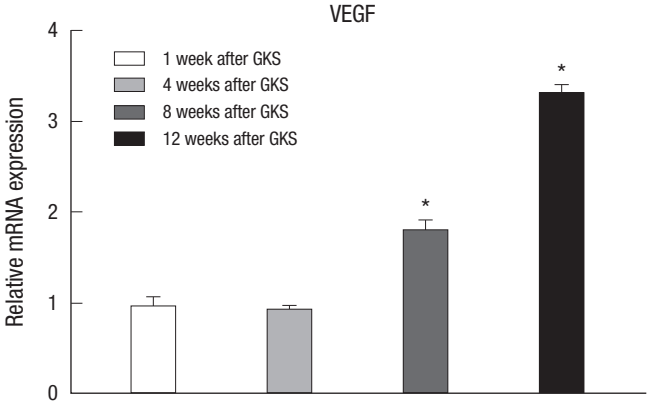

Fig. 5. Quantitative PCR analysis for VEGF in the cortex ipsilateral to the irradiation at 1, 4, 8, and 12 weeks after GKS. The average mRNA expression level in the sham brains was set to 1. Histogram and bars represent the mean ± SD of three replicas. *$P < 0.001$ compared with the sham group.

Association between EMMPRIN and VEGF expression in the parietal cortex after GKS

To further understand the relationship between EMMPRIN and VEGF expression in the irradiated brain, we used a double-immunofluorescence technique to investigate whether EMMPRIN co-localized with VEGF. There were a few EMMPRIN-positive cells (Fig. 7) in the control group, and these cells were not immunopositive for VEGF (Fig. 7). However, EMMPRIN staining colocalized with VEGF staining in the vascular lumen-like structure in the GKS group at 12 weeks after GKS (Fig. 7F). In addition, VEGF expression significantly correlated with EMMPRIN expression by linear regression correlation analysis ($R^2 = 0.822$, $P < 0.001$). These data suggested that enhanced expression of

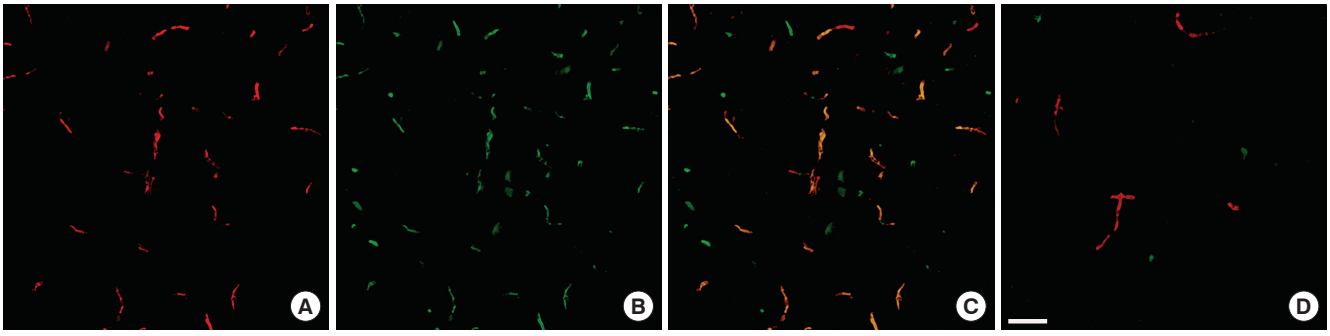

Fig. 6. Representative microphotographs of immunofluorescence double staining for EMMPRIN (red) and caspase-3 immunoreactivity (green) in the target region. Colocalization of EMMPRIN (**A**) and caspase-3 (**B**) was observed in the irradiated cortex following GKS. **C** is a merged image of **A** and **B**. No double-labeling was found in the control groups (**D**). Scale bar = 50 μm.

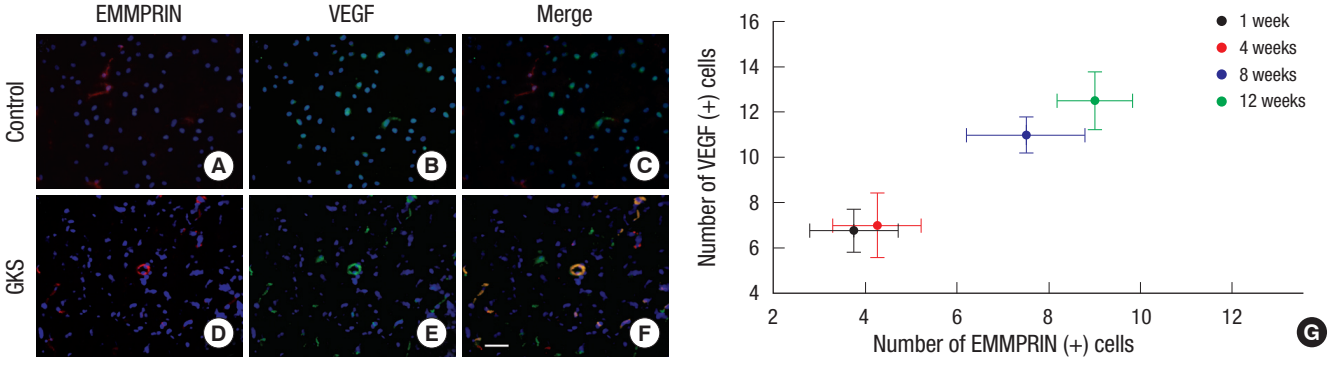

Fig. 7. Relationship between EMMPRIN levels and VEGF expression. (**A**-**F**) Immunofluorescence double staining for EMMPRIN (red) and VEGF immunoreactivity (green) in the target region at 12 weeks after radiosurgery. Double-labeling of EMMPRIN-immunopositive cells (**A**) with VEGF (**B**) was not observed in the sham-operated control cortex (**C**), whereas the colocalization of EMMPRIN (**D**) with VEGF (**E**) was observed in the irradiated cortex (**F**, yellow). Scale bar = 50 μm. (**G**) Correlation between EMMPRIN-positive cells and VEGF expression in the irradiated cortex after GKS.

http://dx.doi.org/10.3346/jkms.2012.27.3.291

EMMPRIN may increase VEGF levels in irradiated brain tissues.

DISCUSSION

Using Gamma Unit C model of the Leksell stereotactic system, irradiation of the right parietal cortex was accomplished, and the targeting accuracy was confirmed (17). According to published radiobiological studies, an intermediate dose of focal gamma-irradiation elicits vascular alterations at 3 months post-irradiation without necrosis (17). Similar results were observed in the present study, in which rats subjected to experimental GKS showed structural and functional changes in the cerebral microvasculature, including the dilation of vessels, morphological damage to endothelial cells and perivascular elements, and an increase in vascular permeability. These vascular injuries may be closely related to increased matrix degradation in the vessel walls and overstimulation of proangiogenic factors in the injured tissue (18).

Data revealed that EMMPRIN expression significantly increased in the irradiated rat cortex after GKS, indicating that EMMPRIN was likely to be correlated with radiation injury after GKS. Although there have been no reported studies to investigate EMMPRIN expression in normal brain tissue after radiosurgery or traditional radiotherapy, EMMPRIN expression has been found in many types of normal tissues, including the brain. On a cellular level, EMMPRIN is identified on the surface of cultured endothelial cells, suggesting that this molecule may play a role in angiogenic function (19). In the normal central nervous system(CNS) tissues, EMMPRIN has been found in endothelial cells and has been linked to CNS regulation and functions such as embryonal blood-brain barrier development and integrin-mediated adhesion in brain endothelia (20). Moreover, most studies have concentrated on the effect of EMMPRIN on pathological conditions because its apparent upregulation is observed in a wide variety of fatal diseases, such as malignant tumors, cerebrovascular disease, and heart disease. A recent study demonstrated that ischemia-induced EMMPRIN expression might contribute to neurovascular remodeling in a mouse model of permanent middle cerebral artery occlusion (8). Excessive expression of EMMPRIN has also been associated with damage of the basal lamina following transient ischemia (21). In addition, previous researchers have found that the EMMPRIN molecule is highly expressed on the surface of various malignant tumor cells and have aimed at the role of EMMPRIN during pathological angiogenesis in these cancers (22). The functional importance of EMMPRIN in pathological conditions has been related mainly to its ability to induce proteases such as MMPs (23) and the urokinase-type plasminogen activation system (uPA) (24). Normally, proteases are thought to represent a key role in ECM degradation and remodeling, which are essential for angiogenesis. However, proteases have been reported to contribute to caspase-mediated brain endothelial cell death (25). Furthermore, proteolytic breakdown of the blood-brain barrier (BBB) vasculature also increases the permeability of the barrier resulting in vasogenic edema and is thought to play an active part in the pathophysiology of CNS diseases (26). In the present study, EMMPRIN- immunopositive cells were double-immunopositive for caspase-3, a major apoptotic factor, in the injured cortex following GKS. Increased EMMPRIN may not only be an initial factor leading to endothelial injury but also a parameter of advanced destruction in apoptotic cells through the stimulation of protease production. The increase of EMMPRIN in irradiated brain tissues (2.9 times higher than in the sham-treated animals) would very likely contribute to the abnormalities in vascular architecture and increased vascular permeability beyond its normal physiological role and eventually lead to disturbed blood flow, metabolic disruptions, and histological changes.

Here, we showed that VEGF expression was also induced by radiosurgery in the normal radiated brain in the subacute stage, reaching maximum levels at 12 weeks after radiosurgery. The pattern of mRNA expression levels in irradiated tissues was similar to that of protein expression levels. The maximum expression of VEGF coincided with both the peak in brain edema and the EB extravasation ratio. The temporal and spatial association of increased VEGF protein expression and vascular lesions suggests that VEGF upregulation is associated with an increase in vascular permeability and edema resulting from GKS injury. This is similar to the findings of a previous conventional radiotherapy study in which VEGF expression in the spinal cord was present at 16-20 weeks after irradiation with 22 Gy, a time at which significant blood-spinal cord barrier breakdown is observed (27). Interestingly, VEGF colocalized with EMMPRIN expressed on endothelial-like cells, and changes in VEGF expression were significantly correlated with EMMPRIN levels in the injured brain of rats receiving GKS. Although the biological and clinical significance of the overexpression of VEGF and EMMPRIN is unclear, the deleterious role of coexpression of VEGF and EMMPRIN has been indicated by the correlation with primary tumors and metastatic rates as well as the poor prognosis for patients with specific malignant tumors. Those patients with VEGF+/EMMPRIN+ co-expression showed significantly shorter overall survival and disease-free survival compared with those of VEGF-/EMMPRIN- expression (28). EMMPRIN-mediated VEGF production likely occurs at different levels, and as noted previously, the increased EMMPRIN in tumor cells is also thought to upregulate VEGF expression in these cells and promote tumor angiogenesis (29). EMMPRIN can also promote angiogenesis by a direct effect on endothelial cells through a regulation of the VEGF/VEGF-receptor (VEGFR) system (30). Although evidence thus far is limited to correlative expression patterns, a direct involvement of EMMPRIN in the regulation of VEGF in irradiated brain tissues seems likely and warrants further investigation. Moreover, it is not entirely

clear how VEGF operates in synergy with EMMPRIN. It is tempting to hypothesize that EMMPRIN might not only provide the support to degrade the extracellular matrix in the radiated brain tissue but also induce BBB permeability and aggravate the radiation-induced vessel injury by upregulating VEGF expression in the target region after GKS. This represents one of the possible mechanisms underlying radiation injury following GKS.

In summary, this is the first study to examine the role of EMMPRIN in CNS radiation injury. Although we cannot exclude the possibility that EMMPRIN has other functions within the CNS post-irradiation, our results suggest that the increases in EMMPRIN and VEGF might be at least partially related to vascular damage after GKS. Future studies should focus on how to modulate the combined action of EMMPRIN and VEGF during the different phases of radiation injury.

ACKNOWLEDGMENTS

The authors sincerely appreciate Shizhu Yu, Yanhe Li, Guokai Wang, Yifeng Cheng, and Youlin Ge, the Second Hospital of Tianjin Medical University, for excellent technical support.

REFERENCES

1. Buis DR, Meijer OW, van den Berg R, Lagerwaard FJ, Bot JC, Slotman BJ, Vandertop WP. *Clinical outcome after repeated radiosurgery for brain arteriovenous malformations. Radiother Oncol 2010; 95: 250-6.*
2. Dewan S, Norén G. *Retreatment of vestibular schwannomas with Gamma Knife surgery. J Neurosurg 2008; 109: 144-8.*
3. Yuan H, Gaber MW, McColgan T, Naimark MD, Kiani MF, Merchant TE. *Radiation-induced permeability and leukocyte adhesion in the rat blood-brain barrier: modulation with anti-ICAM-1 antibodies. Brain Res 2003; 969: 59-69.*
4. Gabison EE, Hoang-Xuan T, Mauviel A, Menashi S. *EMMPRIN/CD147, an MMP modulator in cancer, development and tissue repair. Biochimie 2005; 87: 361-8.*
5. Tang Y, Kesavan P, Nakada MT, Yan L. *Tumor-stroma interaction: positive feedback regulation of extracellular matrix metalloproteinase inducer (EMMPRIN) expression and matrix metalloproteinase-dependent generation of soluble EMMPRIN. Mol Cancer Res 2004; 2: 73-80.*
6. Kato N, Yuzawa Y, Kosugi T, Hobo A, Sato W, Miwa Y, Sakamoto K, Matsuo S, Kadomatsu K. *The E-selectin ligand basigin/CD147 is responsible for neutrophil recruitment in renal ischemia/reperfusion. J Am Soc Nephrol 2009; 20: 1565-76.*
7. Seizer P, Ochmann C, Schönberger T, Zach S, Rose M, Borst O, Klingel K, Kandolf R, Macdonald HR, Nowak RA, Engelhardt S, Lang F, Gawaz M, May AE. *Disrupting the EMMPRIN (CD147)-cyclophilin A interaction reduces infarct size and preserves systolic function after myocardial ischemia and reperfusion. Arterioscler Thromb Vasc Biol 2011; 31: 1377-86.*
8. Zhu W, Khachi S, Hao Q, Shen F, Young WL, Yang GY, Chen Y. *Upregulation of EMMPRIN after permanent focal cerebral ischemia. Neurochem Int 2008; 52: 1086-91.*
9. Nahalkova J, Volkmann I, Aoki M, Winblad B, Bogdanovic N, Tjernberg LO, Behbahani H. *CD147, a gamma-secretase associated protein is upregulated in Alzheimer's disease brain and its cellular trafficking is affected by presenilin-2. Neurochem Int 2010; 56: 67-76.*
10. Agrawal SM, Silva C, Tourtellotte WW, Yong VW. *EMMPRIN: a novel regulator of leukocyte transmigration into the CNS in multiple sclerosis and experimental autoimmune encephalomyelitis. J Neurosci 2011; 31: 669-77.*
11. Menashi S, Serova M, Ma L, Vignot S, Mourah S, Calvo F. *Regulation of extracellular matrix metalloproteinase inducer and matrix metalloproteinase expression by amphiregulin in transformed human breast epithelial cells. Cancer Res 2003; 63: 7575-80.*
12. Gabison EE, Mourah S, Steinfels E, Yan L, Hoang-Xuan T, Watsky MA, De Wever B, Calvo F, Mauviel A, Menashi S. *Differential expression of extracellular matrix metalloproteinase inducer (CD147) in normal and ulcerated corneas: role in epithelio-stromal interactions and matrix metalloproteinase induction. Am J Pathol 2005; 166: 209-19.*
13. Dent P, Yacoub A, Contessa J, Caron R, Amorino G, Valerie K, Hagan MP, Grant S, Schmidt-Ullrich R. *Stress and radiation-induced activation of multiple intracellular signaling pathways. Radiat Res 2003; 159: 283-300.*
14. Criscuolo GR. *The genesis of peritumoral vasogenic brain edema and tumor cysts: a hypothetical role for tumor-derived vascular permeability factor. Yale J Biol Med 1993; 66: 277-314.*
15. Zhang ZG, Zhang L, Jiang Q, Zhang R, Davies K, Powers C, Bruggen N, Chopp M. *VEGF enhances angiogenesis and promotes blood-brain barrier leakage in the ischemic brain. J Clin Invest 2000; 106: 829-38.*
16. Li YQ, Ballinger JR, Nordal RA, Su ZF, Wong CS. *Hypoxia in radiation-induced blood-spinal cord barrier breakdown. Cancer Res 2001; 61: 3348-54.*
17. Kamiryo T, Kassell NF, Thai QA, Lopes MB, Lee KS, Steiner L. *Histological changes in the normal rat brain after gamma irradiation. Acta Neurochir (Wien) 1996; 138: 451-9.*
18. Fedak PW, de Sa MP, Verma S, Nili N, Kazemian P, Butany J, Strauss BH, Weisel RD, David TE. *Vascular matrix remodeling in patients with bicuspid aortic valve malformations: implications for aortic dilatation. J Thorac Cardiovasc Surg 2003; 126: 797-806.*
19. Chen Y, Zhang H, Gou X, Horikawa Y, Xing J, Chen Z. *Upregulation of HAb18G/CD147 in activated human umbilical vein endothelial cells enhances the angiogenesis. Cancer Lett 2009; 278: 113-21.*
20. Seulberger H, Unger CM, Risau W. *HT7, neurothelin, basigin, gp42 and OX-47: many names for one developmentally regulated immuno-globulin-like surface glycoprotein on blood–brain barrier endothelium, epithelial tissue barriers and neurons. Neurosci Lett 1992; 140: 93-7.*
21. Burggraf D, Liebetrau M, Martens HK, Wunderlich N, Jäger G, Dichgans M, Hamann GF. *Matrix metalloproteinase induction by EMMPRIN in experimental focal cerebral ischemia. Eur J Neurosci 2005; 22: 273-7.*
22. Tang Y, Nakada MT, Kesavan P, McCabe F, Millar H, Rafferty P, Bugelski P, Yan L. *Extracellular matrix metalloproteinase inducer stimulates tumor angiogenesis by elevating vascular endothelial cell growth factor and matrix metalloproteinases. Cancer Res 2005; 65: 3193-9.*
23. Huet E, Gabison EE, Mourah S, Menashi S. *Role of emmprin/CD147 in tissue remodeling. Connect Tissue Res 2008; 49: 175-9.*
24. Quemener C, Gabison EE, Naïmi B, Lescaille G, Bougatef F, Podgorniak MP, Labarchède G, Lebbé C, Calvo F, Menashi S, Mourah S. *Extracellular matrix metalloproteinase inducer up-regulates the urokinase-type plasminogen activator system promoting tumor cell invasion. Cancer*

 http://dx.doi.org/10.3346/jkms.2012.27.3.291

Res 2007; 67: 9-15.

25. Lee SR, Lo EH. *Induction of caspase-mediated cell death by matrix metalloproteinases in cerebral endothelial cells after hypoxia-reoxygenation. J Cereb Blood Flow Metab 2004; 24: 720-7.*
26. Gasche Y, Copin JC, Sugawara T, Fujimura M, Chan PH. *Matrix metalloproteinase inhibition prevents oxidative stress-associated blood-brain barrier disruption after transient focal cerebral ischemia. J Cereb Blood Flow Metab 2001; 21: 1393-400.*
27. Tsao MN, Li YQ, Lu G, Xu Y, Wong CS. *Upregulation of vascular endothelial growth factor is associated with radiation-induced blood-spinal cord barrier breakdown. J Neuropathol Exp Neurol 1999; 58: 1051-60.*
28. Zhou Q, Zhu Y, Deng Z, Long H, Zhang S, Chen X. *VEGF and EMMPRIN expression correlates with survival of patients with osteosarcoma. Surg Oncol 2011; 20: 13-9.*
29. Tang Y, Nakada MT, Kesavan P, McCabe F, Millar H, Rafferty P, Bugelski P, Yan L. *Extracellular matrix metalloproteinase inducer stimulates tumor angiogenesis by elevating vascular endothelial cell growth factor and matrix metalloproteinases. Cancer Res 2005; 65: 3193-9.*
30. Bougatef F, Quemener C, Kellouche S, Naïmi B, Podgorniak MP, Millot G, Gabison EE, Calvo F, Dosquet C, Lebbé C, Menashi S, Mourah S. *EMMPRIN promotes angiogenesis through hypoxia-inducible factor-2alpha-mediated regulation of soluble VEGF isoforms and their receptor VEGFR-2. Blood 2009; 114: 5547-56.*